Periodic orbit theory for realistic cluster potentials

Erik Koch
Max-Planck-Institut für Festkörperforschung, D-70569 Stuttgart, Germany
(Received 9 January 1998)

The formation of supershells observed in large metal clusters can be qualitatively understood from a periodic orbit expansion for a spherical cavity. To describe the changes in the supershell structure for different materials, one has, however, to go beyond that simple model. We show how periodic orbit expansions for realistic cluster potentials can be derived by expanding *only* the classical radial action around the limiting case of a spherical potential well. We give analytical results for the leptodermous expansion of Woods-Saxon potentials, and show that it describes the shift of the supershells as the surface of a cluster potential becomes softer. [S0163-1829(98)03327-X]

I. INTRODUCTION

One of the most surprising aspects of the physics of metal clusters is the supershell structure observed in mass-abundance spectra.[1–4] This feature can be traced back to a beating pattern in the density of states for typical cluster potentials.[5] The conceptual framework for understanding how this quantum interference comes about is provided by periodic orbit theory.[6,7] The elegance of this approach rests on the fact that the periodic orbit expansion (POE) is known analytically for the spherical cavity. For this model potential it was found that the most important contributions to the oscillating part of the density of states stem from the two shortest planar periodic orbits: triangular and square orbits. Since these contributions oscillate with similar frequencies, their interference gives rise to a beating pattern, hence supershells.

Although a spherical potential well is a good first approximation to a cluster potential, this model clearly cannot account for the changes in the electronic shell and supershell structure observed for clusters made of different materials. It is therefore desirable to understand how the periodic orbit expansion is modified as one considers more realistic model potentials. A straightforward approach for doing so is to solve the action integrals, which lie at the heart of periodic orbit theory, numerically. That way, however, most of the elegance and power of the periodic orbit expansion is lost. An analytical expression, on the other hand, may well reveal the relevant parameters determining the supershell structure, and provide insight into how it changes as the cluster potential is varied. They should prove especially helpful in the search for better self-consistent models, which properly describe the experimental data.

While the simple spherical, homogeneous jellium model[8,9] works quite well for the alkali clusters, it fails to describe the supershell structure observed in Ga_N.[4] Attempts to improve the situation include, e.g., the introduction of smooth jellium profiles,[10] the inclusion of pseudopotentials,[11–13] or the consideration of surface roughness.[14]

The present work arises from the desire to understand the simple spherical, homogeneous jellium model. An analysis of the density dependence of the electronic supershells in jellium clusters showed that the supershells are shifted as the potential at the cluster surface becomes softer.[15] It has been demonstrated that this shift can be understood in the framework of a periodic orbit expansion for typical self-consistent cluster potentials.[16] The purpose of the present paper is to give a derivation of the leptodermous expansion, which requires the linearization of *only the radial action*. We furthermore analyze the validity of the approximations involved, and show comparisons with quantum-mechanical calculations.

To set the stage for the semiclassical treatment of electronic supershells, Sec. II gives a review of the shell correction methods.[17–19] These methods establish a systematic relation between self-consistent calculations and one-electron calculations for suitable model potentials. We stress the fact that it is decisive to choose families of potentials that vary smoothly with cluster size, to describe the electronic shell structure properly.

Section III is devoted to periodic orbit expansions. We sketch the derivation of the POE for the oscillating part $\tilde{\rho}$ of the density of states using the path-integral formalism along the lines given by Gutzwiller.[7] Special attention is paid to the rate of convergence of the sum over classical periodic orbits. Since the shell and supershell structure observed in the mass spectra of metal clusters are not directly linked to $\tilde{\rho}$ but rather the variations $\tilde{E}$ in *total energy*, we proceed to derive a periodic orbit expansion for $\tilde{E}$. We find that the latter expansion converges much more rapidly than that for the density of states, hence making any artificial smoothing of the spectrum, commonly introduced to lessen the contribution of the longer orbits to $\tilde{\rho}$,[6,5,20] superfluous. To assess the validity of the expression for $\tilde{E}$, we check the truncated POE against the quantum-mechanical result. This comparison shows that in the size range, which seems experimentally accessible, $\tilde{E}$ is well described by a truncated POE, taking only triangular and square orbits into account. This justifies the common practice of truncating the POE after the two shortest *planar* orbits.

In Sec. IV we show how to extend the periodic orbit expansion of $\tilde{E}$ to more realistic potentials. We start from the observation that the surface width a of the cluster potential is an important parameter determining the supershell structure.[15] The basic idea is then to expand the action integrals entering the POE around the analytically known results

 © 1998 The American Physical Society

for a potential well. It turns out that the actions can be very well approximated by linear functions in the surface parameter a/R_0, where R_0 is the radius of the cluster. Thus a finite surface width leaves the frequencies in the POE unchanged and, to first order, only introduces phase shifts. Taking also the change of the Fermi energy into account, we can understand the changes in the electronic shells and supershells introduced by a soft potential surface. The technical details of the leptodermous expansion for Woods-Saxon potentials are described in the Appendix. To simplify the notation, we set $\hbar^2/2m$ to unity, i.e., we give lengths in Bohr radii (a_0), and energies in Rydberg.

II. SHELL CORRECTION METHODS

The total energy $E(N)$ of clusters having N valence electrons can be split into smooth and oscillating parts:

$$E(N)=\overline{E}(N)+\tilde{E}(N). \tag{1}$$

The smooth part describes the overall change in energy as the cluster size increases, and is given by a liquid drop expansion[21,22]

$$\overline{E}(N)=a_1N+a_2N^{2/3}+a_3N^{1/3}+\cdots. \tag{2}$$

The oscillating part is responsible for the shell structure.

The idea of shell correction methods is to give a prescription for determining $\tilde{E}(N)$ from a one-particle calculation. These methods were pioneered by Strutinsky and coworkers, who showed how the oscillating part of the total energy resulting from a Hartree-Fock calculation for atomic nuclei can be determined from the sum of the single-particle energies $\Sigma\epsilon_\mu$ of a suitably defined potential.[17,18] A similar result holds for $\tilde{E}(N)$ extracted from local-density-functional calculations.[19] The latter are more common for metal clusters.[9,23,24] For clarity, and to fix the notation, we give a short outline of the relevant argument.

To find the ground-state energy of a system of N electrons using density-functional theory, we use the Kohn-Sham formalism.[25,26] Starting from some electron density $n_0(r)$ we have to solve the Kohn-Sham equations with the potential

$$V_{KS}(\vec{r})=V_{ext}(\vec{r})+\int d^3r'\,\frac{n_0(\vec{r}')}{|\vec{r}-\vec{r}'|}+V_{xc}[n_0]. \tag{3}$$

Having found the N lowest eigenstates $\psi_\mu(\vec{r})$ with energies ϵ_μ, an estimate of the total energy of the system is given by the variational expression

$$E[n_0]=E_{kin}[n_0]+E_{Coul}[n_0]+E_{xc}[n_0], \tag{4}$$

where the kinetic energy is given by

$$E_{kin}[n_0]=\sum_{\mu=1}^{N}\epsilon_\mu-\int d^3r\;d^3r'\,\frac{n_0(\vec{r})n(\vec{r})}{|\vec{r}-\vec{r}'|}-\int d^3rV_{xc}[n_0]n(\vec{r})-\int d^3rV_{ext}(\vec{r})n(\vec{r}), \tag{5}$$

and the Coulomb energy is the sum of the Hartree energy, the interaction of the electron density with the external potential (e.g., the potential arising for the ion cores), and the electrostatic self-energy of the ionic cores

$$E_{Coul}[n_0]=\frac{1}{2}\int d^3r\;d^3r'\,\frac{n(\vec{r})n(\vec{r}')}{|\vec{r}-\vec{r}'|}+\int d^3rV_{ext}(\vec{r})n(\vec{r})+E_I. \tag{6}$$

The ''new'' electron density $n(\vec{r})$ in the above expressions is given by $\Sigma_\mu|\psi_\mu(\vec{r})|^2$.

Let us assume that $n_0(\vec{r})$ was chosen close to self-consistency. Then $n(\vec{r})$ will not differ too much from $n_0(\vec{r})$,

$$n(\vec{r})=n_0(\vec{r})+\delta n(\vec{r}), \tag{7}$$

and we can expand the expression for the total energy (4) in powers of δn. Using

$$\frac{1}{2}\int d^3r\;d^3r'\,\frac{nn}{|\vec{r}-\vec{r}'|}=-\frac{1}{2}\int d^3rd^3r'\,\frac{n_0n_0}{|\vec{r}-\vec{r}'|}+\int d^3r\;d^3r'\,\frac{n_0n}{|\vec{r}-\vec{r}'|}+\mathcal{O}^2(\delta n)$$

and

$$E_{xc}[n]=E_{xc}[n_0]+\int d^3r\;\underbrace{\frac{\delta E_{xc}[n_0]}{\delta n}}_{=V_{xc}[n_0](\vec{r})}\delta n(\vec{r})+\mathcal{O}^2(\delta n)$$

we can, to first order in δn, write the total energy as a functional of only the initial electron density $n_0(r)$:

$$E=\sum_\mu\varepsilon_\mu-\frac{1}{2}\int d^3r\;d^3r'\,\frac{n_0(\vec{r})n_0(\vec{r}')}{|\vec{r}-\vec{r}'|}-\int d^3rV_{xc}[n_0](\vec{r})n_0(\vec{r})+E_{xc}[n_0]+E_I. \tag{8}$$

A good choice for n_0 is the electron density n_{TF} resulting from an extended Thomas-Fermi (ETF) calculation. Since $n_{ETF}(N;r)$ varies smoothly as the number of the valence electrons N in the cluster is changed, all terms in Eq. (8), except for the first one, contribute exclusively to the smooth part $\overline{E}(N)$ of the total energy. That is, to first order in δn, all electronic shell effects $\tilde{E}(N)$ are contained in the sum of the one-particle energies $\Sigma\epsilon_\mu$. Hence the oscillating part $\tilde{E}(N)$ of the total energy can be determined from the spectrum of the family $V(N;r)$ of Kohn-Sham potentials which arise from the electron density $n_{ETF}(r)$. More generally, the above

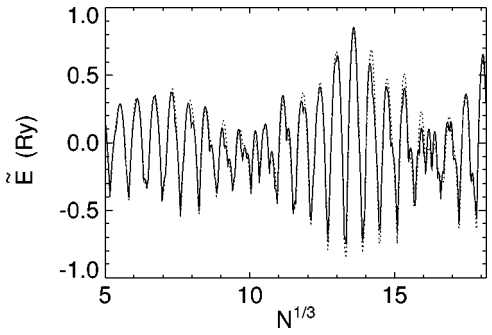

FIG. 1. Comparison of the oscillating part $\tilde{E}(N)$ of the total energy obtained from a self-consistent calculation using the homogeneous spherical jellium model (dotted line) to the $\tilde{E}(N)$ extracted from the sum of the one-particle energies of a family of model potentials (full line). The model potentials are given in Eq. (10), with parameters $r_s=2.19a_0$, $V_0=1.04$ Ry, $\Delta R=0.73a_0$, $a_0=1.03a_0$, $a_1=1.13a_0$, and $a_2=0.21a_0$.

reasoning holds for all *families* of electron densities $n_0(N;r)$ that are close to self-consistency and *smooth in* N.

It is common practice to immediately work with parametrized potentials $V(N;r)$. Usually they are chosen to fit experiments or the results of self-consistent calculations.[27,5,28,10] Imagining that these potentials arise from a hypothetical family of electron densities, the above arguments still apply. The prototype of such a phenomenological shell model is the Woods-Saxon potential[27,5,28]

$$V(N;r)=\frac{-V_0}{1+\exp[(r-r_sN^{1/3})/a]}. \tag{9}$$

Variants are the Wine-bottle potential[5] and the Woods-Saxon potential with asymmetric surface,[10]

$$V(N;r)=\frac{-V_0}{1+\exp\{[r-(r_sN^{1/3}+\Delta R)]/f(r)\}}, \tag{10}$$

where $f(r)$ is an analytical function modeling the potential near the cluster surface.

To get a feeling for the approximations involved, we compare the results of a self-consistent calculation for gallium clusters to the oscillating part of the total energy found using a family of model potentials (Fig. 1). For the self-consistent calculations we used the homogeneous, spherical jellium model.[9] The potentials for the one-particle calculation were obtained by fitting a function of type (10),

$$V(N;r)=\frac{-V_0}{1+\exp[(r-R(N))/a(r)]}, \tag{11}$$

where $R(N)=r_sN^{1/3}+\Delta(r)$ and $a(r)=a_0+a_1\tanh\{[a_2(r-R(N)]\}$, to the self-consistent Kohn-Sham potentials for jellium clusters having 1500, 3000, 4500, and 6000 valence electrons.

To emphasize the importance of the smoothness of the model potentials $V(N;r)$ in N, and to demonstrate from what subtle cancellations the electronic shell structure arises in self-consistent calculations, in Fig. 2 we show the oscillating part of the total, the kinetic, the Coulomb, and the exchange-correlation energy determined from a jellium calculation for gallium clusters. Even though in this calculation we are dealing with the self-consistent potentials and electron densities (i.e., $\delta n=0$), $E_{kin}(N)$, which contains the sum of the Kohn-Sham energies, is by far not the only term contributing to $\tilde{E}(N)$. More surprisingly the electronic shell structure as revealed by $\tilde{E}$ cannot be found in any *single* contributions to the total energy. For the self-consistent calculation, it rather results from the subtle interplay of the different oscillating terms.

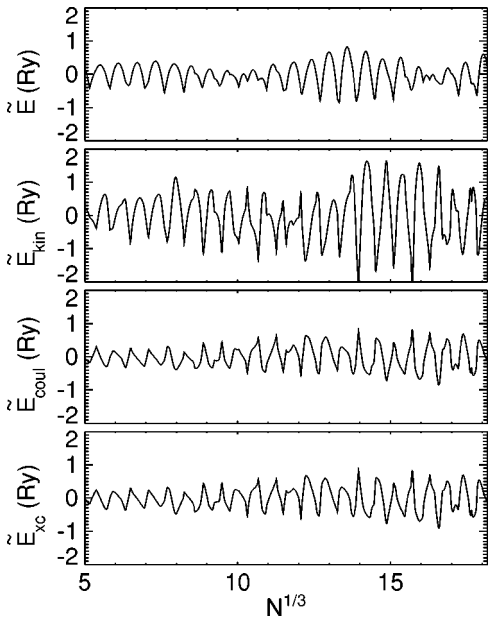

FIG. 2. Oscillating part of the total energy and of contributions to it [cf. Eq. (4)], obtained from a self-consistent calculation using the homogeneous, spherical jellium model.

III. PERIODIC ORBIT EXPANSION (POE)

As we saw in Sec. II, the oscillating part $\tilde{E}$ of the total energy can be extracted from the sum $\Sigma\varepsilon_i$ of the N lowest eigenenergies for a suitably chosen family $V(N;r)$ of model potentials. The determination of the electronic shell and supershell structure is thus reduced to an eigenvalue problem for these potentials. Furthermore, the radius of the clusters we are interested in is considerably larger than the de Broglie wavelength of the electrons at the Fermi level. The semiclassical approximation therefore seems well suited for solving the single-electron problem in question. In fact, for the spherical cavity, a simple rescaling of the Schrödinger equation shows that the limit $R\to\infty$ is identical to the semiclassical limit $\hbar\to 0$.

The salient feature of the semiclassical approach to determining the electronic shell and supershell structure is that it provides a natural splitting of the density of states (and consequently the total energy) into smooth and oscillating parts. The smooth part corresponds to Thomas-Fermi theory, while the quantum corrections are given by a sum over the nontrivial periodic orbits. For an understanding of the oscillating part $\tilde{E}$ of the total energy, we need only consider the latter.

In the present section we derive the POE for spherical potential wells. Starting from the oscillating part $\tilde{\rho}(k)dk$ of

the density of states for a given potential $V(r)$, we proceed to a POE for the oscillating part $\tilde{E}(N)$ of the total energy for a family $V(N;r)$ of potentials. We illustrate the results by giving explicit expressions for infinite potential wells. These will be the points of reference for the leptodermous expansion discussed in Sec. IV. We furthermore use the spherical cavity to assess the validity of the various approximations made, by comparing the semiclassical results to the results obtained from numerically solving the Schrödinger equation.

A. POE for the density of states

The periodic orbit expansion for the density of states $\rho(E)$ can be derived starting from the path-integral representation of the energy-dependent Green's function $G(\vec{r},\vec{r}_0;E)$ by taking the semiclassical limit $\hbar\to 0$.[7,29–31] $\rho(E)$ is then given by

$$\rho(E)dE=-\frac{1}{\pi}\Im\ \mathrm{Tr}G(E+i\epsilon)dE. \tag{12}$$

In the semiclassical limit $G(\vec{r},\vec{r}_0;E)$ is given by a sum over classical paths. Taking the trace of $G(\vec{r},\vec{r}_0;E)$ involves integrating over $\vec{r}_0$ and taking the limit $\vec{r}\to\vec{r}_0$. The integration is done in the semiclassical limit. The stationary-phase condition then requires that the final moment along the classical path equals the initial moment. The limit $\vec{r}\to\vec{r}_0$ closes the paths. Thus, since the paths return to $\vec{r}_0$ with the same momentum, they are closed in phase space, i.e., they are periodic. There are two distinct classes of such orbits. The first consists of only the *direct path*, the length of which vanishes as $\vec{r}\to\vec{r}_0$. It consequently is *local* and gives rise to the Thomas-Fermi density of states $\overline{\rho}$. The second class consists of periodic orbits of finite length. These *nonlocal* paths give rise to a quantum correction to $\overline{\rho}$. Hence in the semiclassical approximation the density of states is given by the local Thomas-Fermi term with nonlocal corrections described by a sum over periodic orbits:

$$\rho(E)dE=[\overline{\rho}(E)+\tilde{\rho}(E)]dE. \tag{13}$$

In a spherical potential well, i.e., a potential with at most two radial turning points, all periodic orbits can be easily enumerated: A periodic orbit is characterized by the number λ of times it winds around the origin, and the number ν of times it traverses the outer turning point. By symmetry all orbits (λ,ν) that only differ in orientation are equivalent. Figure 3 shows some of the periodic orbits for a spherical cavity. The periodic orbits for a general spherical potential well are more rounded, but are still described by the pairs (λ,ν).[5,32] The periodic orbit expansion for the oscillating part of the density of states is thus given by a sum over the families of equivalent orbits (λ,ν),

$$\tilde{\rho}(E)dE=\sum_{(\lambda,\nu)}A_{(\lambda,\nu)}\cos\left(\frac{S_{(\lambda,\nu)}}{\hbar}-\varphi_{(\lambda,\nu)}\right)dE, \tag{14}$$

where $S_{(\lambda,\nu)}$ is the classical action for an orbit (λ,ν), and $\varphi_{(\lambda,\nu)}$ is the Maslov phase. The amplitude with which the orbit (λ,ν) contributes is given by

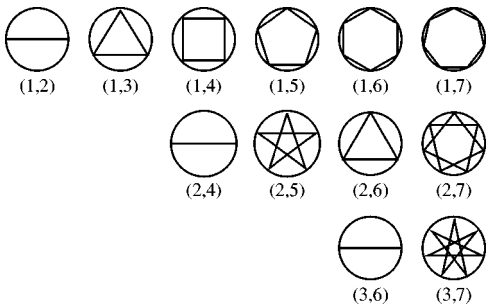

FIG. 3. Some periodic orbits for a spherical cavity. They are characterized by the pair (λ,ν), where λ denotes the number of times the orbit revolves around the origin before it closes on itself, and ν is the number of vertices it has. Note that $(n\lambda,n\nu)$ is the orbit obtained by traversing (λ,ν) n times.

$$A_{(\lambda,\nu)}=\frac{4}{\sqrt{\pi\nu}}\frac{L_{(\lambda,\nu)}}{\hbar}\frac{\partial s_r/\hbar}{\partial E}\left|\frac{\partial^2 s_r\hbar}{\partial L^2}\right|^{-1/2}, \tag{15}$$

with L denoting the angular momentum and s_r the radial action.[7]

For a spherical cavity of radius R_0, the terms that enter the periodic orbit expansion take a simple form: The classical action of an orbit equals its length times the wave vector k,

$$S_{(\lambda,\nu)}(k)/\hbar=2\nu kR_0\sin\left(\frac{\pi\lambda}{\nu}\right); \tag{16}$$

the phase is given by

$$\varphi_{(\lambda,\nu)}=\left(\frac{3}{2}\nu+\lambda-\frac{1}{4}\right)\pi; \tag{17}$$

and the amplitude takes the form

$$A_{(\lambda,\nu)}=\sqrt{k}R_0^{5/2}\alpha_{(\lambda,\nu)}, \tag{18}$$

with the dimensionless geometry factors

$$\alpha_{(\lambda,\nu)}=\frac{2}{\sqrt{\pi\nu}}\sqrt{\sin\left(\frac{\pi\lambda}{\nu}\right)}\sin\left(\frac{2\pi\lambda}{\nu}\right). \tag{19}$$

The $\alpha_{(\lambda,\nu)}$'s determine the relative importance of the periodic orbits in the POE [Eq. (14)]. Their values for the first few periodic orbits are shown in Fig. 4 $(k_i=0)$. We note that the amplitudes for the linear orbits $(\lambda,2\lambda)$ vanish. This can be understood by a simple dimensional argument.[6] Since the sum in the POE is over *all* periodic orbits, the number of different but equivalent orbits (λ,ν) will be reflected in the amplitude $\alpha_{(\lambda,\nu)}$. To parametrize all the different orientations of the linear orbits, it is sufficient to give the coordinates of one of their outer turning points. Since for a spherical potential well the outer turning point lies on the surface of a sphere, the manifold of the linear orbits has dimension 2. All the higher orbits are not linear but lie in a plane, so we need an additional parameter to fix the orientation of this plane. The manifold of the planar orbits are therefore three-dimensional (''there are many more planar than linear orbits''). Thus the linear orbits do not contribute to the leading order of the periodic orbit expansion. The largest amplitudes are found for the triangular (1,3) and the square (1,4) orbit.

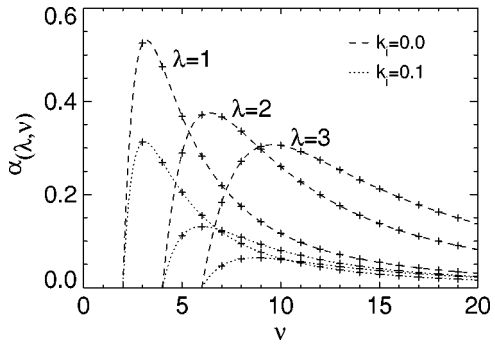

FIG. 4. Amplitudes $\alpha_{(\lambda,\nu)}$ with which the periodic orbits (λ,ν) contribute to the oscillating part $\tilde{\rho}$ of the density of states. Shown are the amplitudes (crosses) for no ($k_i=0$) and for an intermediate ($k_i=0.1$) smoothing. To guide the eye, the amplitudes for a given number of turns are connected by lines.

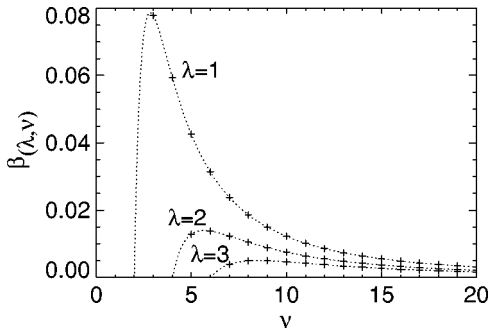

FIG. 5. Amplitudes $\beta_{(\lambda,\nu)}$ with which the periodic orbits (λ,ν) contribute to the oscillating part $\tilde{E}$ of the total energy. Comparison with Fig. 4 shows that the dominance of the short, planar orbits, which for the oscillating part $\tilde{\rho}$ of the density of states has to be enforced by introducing an artificial smoothing k_i, occurs naturally for $\tilde{E}$.

The contribution from other orbits is, however, still large, i.e., one has to include many periodic orbits in a partial summation of Eq. (14) before one obtains a result close to $\tilde{\rho}$. This slow convergence is to be expected since the density of states for a finite system is given by a sum of δ functions which cannot easily be reproduced by a sum of analytical functions. To improve the convergence of the expansion, one can replace the δ peaks in the density of states by Lorentzians of width γ. This corresponds to introducing a complex wave vector $k=k_r+ik_i$ in the periodic orbit expansion. As can be seen from Fig. 4, a finite value of k_i serves to reduce the contribution of higher orbits considerably. However, since the shell and supershell structures in metal clusters are not directly linked to $\tilde{\rho}$ but rather to the variations $\tilde{E}$ in the total energy, we proceed to derive a periodic orbit expansion for $\tilde{E}$. As we will see, such an expansion converges much more rapidly than that for the density of states. We therefore need not introduce any smoothing.

B. POE for the total energy

To find a periodic orbit expansion for the oscillating part $\tilde{E}$ of the total energy using the POE for $\tilde{\rho}$, we start from the integral

$$E(N)=\int_0^{E_F(N)} E\rho(N;E)dE, \tag{20}$$

where the Fermi energy $E_F(N)$ is fixed by the number of electrons N in the cluster,

$$N=\int_0^{E_F(N)} \rho(N;E)dE. \tag{21}$$

Similar equations hold in Thomas-Fermi theory. Subtracting the corresponding Thomas-Fermi expression from Eq. (21), we find

$$0=\int_{\overline{E}_F(N)}^{E_F(N)} \overline{\rho}(N;E)dE+\int_0^{E_F(N)} \tilde{\rho}(N;E)dE. \tag{22}$$

Since the smooth part of the density of states does not vary much over the small interval $\overline{E}_F,\ldots,E_F$, we can approximate the first integral in the above expression by $\tilde{E}_F(N)\overline{\rho}(N;E_F)$. We then can use the above equation to solve for $\tilde{E}_F(N)$. In a similar fashion we can approximate the difference of Eq. (20) and its Thomas-Fermi counterpart by

$$\tilde{E}(N)\approx\tilde{E}_F(N)E_F(N)\overline{\rho}(N;E_F)+\int_0^{E_F(N)} E\tilde{\rho}(N;E)dE.$$

Using the approximate expression for $\tilde{E}_F$ from Eq. (22), we find

$$\tilde{E}(N)\approx\int_0^{E_F(N)}[E-E_F(N)]\tilde{\rho}(N;E)dE. \tag{23}$$

Since the integrand vanishes at the upper limit of integration it is now possible to approximate $E_F(N)$ by its Thomas-Fermi counterpart $\overline{E}_F(N)$. Integrating by parts, we finally arrive at

$$\tilde{E}(N)\approx-\int_0^{\overline{E}_F(N)} dE\int_0^{E} dE'\tilde{\rho}(N;E'), \tag{24}$$

i.e., to find an approximation to the oscillating part of the total energy we have to integrate twice over the oscillating part of the density of states.

Using Eqs. (24) and (14), we find, for spherical cavities of radius $R_0(N)$, the expansion

$$\tilde{E}(N)\approx\sqrt{\overline{k}_F R_0}\overline{k}_F^2\sum_{(\lambda,\nu)}\frac{4\alpha_{(\lambda,\nu)}}{\hat{S}^2_{(\lambda,\nu)}}\cos(\hat{S}_{(\lambda,\nu)}\overline{k}_F R_0-\varphi_{(\lambda,\nu)}) \tag{25}$$

which is similar to Eq. (14), the main difference being the change in the amplitudes: Due to the twofold integration the amplitudes are divided by the square of the dimensionless classical action $\hat{S}_{(\lambda,\nu)}=S_{(\lambda,\nu)}/(\hbar k R_0)$. The new geometry factors are thus given by

$$\beta_{(\lambda,\nu)}:=\frac{4\alpha_{(\lambda,\nu)}}{\hat{S}^2_{(\lambda,\nu)}}. \tag{26}$$

They are plotted in Fig. 5. A comparison with $\alpha_{(\lambda,\nu)}$ (Fig. 4) shows how the contributions of the long orbits [with large

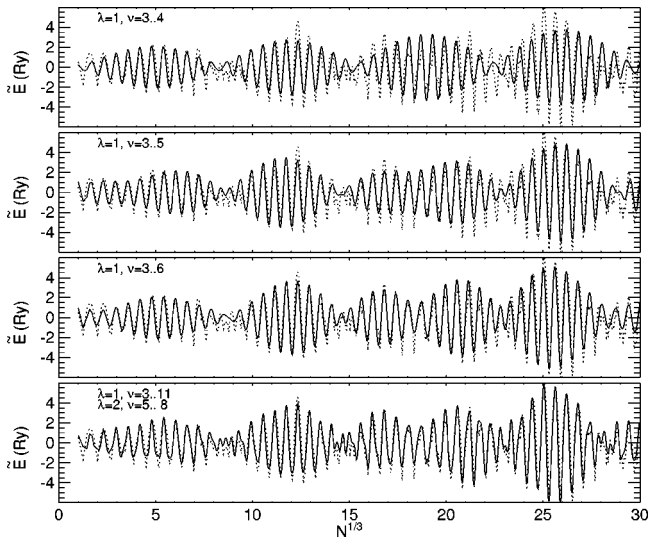

FIG. 6. Comparison of the periodic orbit expansion for the oscillating part $\tilde{E}$ of the total energy to the quantum-mechanical result for spherical cavities. The plots show $\tilde{E}$ obtained from a truncated periodic orbit expansion, including more and more orbits. The orbits were included in the order of decreasing amplitude: (1,3), (1,4), (1,5), (1,6), (1,7), (1,8), (1,9), (2,6), (2,5), (2,7), (1,10), (2,8), and (1,11). $\tilde{E}_{QM}$ from the quantum-mechanical calculation is shown by the dotted line.

classical action; see Eq. (16)] to the POE for $\tilde{E}(N)$ are reduced. This improvement of convergence can be understood intuitively since $E(N)$ is continuous, while the density of states is highly singular, being a forest of δ functions.

To check the approximations made in the derivation of Eq. (24), we compare the results of a truncated periodic orbit expansion for $\tilde{E}$ with the oscillating part $\tilde{E}_{QM}$ of the total energy derived from a quantum-mechanical calculation. Such a comparison for spherical cavities of radius $R_0=N^{1/3}$ is shown in Fig. 6. It turns out that the truncated POE's reproduce $\tilde{E}_{QM}$ very well, even if only a few periodic orbits are included. In particular, the first two supershells can be described using only the triangular and square orbits. However, for even larger sizes N it seems that higher orbits are needed to describe the structure in $\tilde{E}_{QM}$. We note that due to its nature of being a semiclassical result, the periodic orbit expansion for $\tilde{E}$ will not converge to $\tilde{E}_{QM}$ but to its semiclassical approximation.

IV. LEPTODERMOUS EXPANSION

So far we only have explicit expressions of the periodic orbit expansion for cavity potentials. We now want to extend the POE to more realistic potentials $V(r)$, like the Woods-Saxon potential [Eq. (9)]. These potentials differ from the cavity potential by having a surface of finite width a. Since the slope of the cavity potential is infinite at the surface, $\delta V(r)=V(r)-V_{cavity}$ is never a small quantity. But, rewriting integrals over $V(r)$ in a suitable way, we can use the surface width a as an expansion parameter.

From Eq. (25), we see that we need to find expressions for (i) the action integral $\hat{S}_{(\lambda,\nu)}$ for orbits (λ,ν), (ii) the Fermi wave vector $\bar{k}_F$ in the Thomas-Fermi approximation, and (iii) the phases $\varphi_{(\lambda,\nu)}$. For this we proceed as follows. We first introduce the idea of the leptodermous expansion for integrals over the potential $V(r)$ for classical action. We find an expansion

$$\hat{S}_{(\lambda,\nu)}=\hat{S}^{cavity}_{(\lambda,\nu)}+2\nu\hat{I}_s\frac{a}{R_0}. \tag{27}$$

Then we estimate the change in $\bar{k}_F r_s$ due to the finite surface width. To first order in a, we find

$$\bar{k}_F r_s=\left(\frac{9\pi}{4}\right)^{1/3}+\left(c_1+c_2\frac{a}{r_s}\right)N^{-1/3}. \tag{28}$$

Finally we estimate the phase $\varphi_{(\lambda,\nu)}$. Rearranging terms in powers of $N^{1/3}$, the argument of the cosine in Eq. (25) then reads

$$\left(\frac{9\pi}{4}\right)^{1/3}\hat{S}^{cavity}_{(\lambda,\nu)}N^{1/3}+\hat{S}^{cavity}_{(\lambda,\nu)}\left(c_1+c_2\frac{a}{r_s}\right)+2\nu\left(\frac{9\pi}{4}\right)^{1/3}\hat{I}_s\frac{a}{r_s}-\varphi_{(\lambda,\nu)}, \tag{29}$$

i.e., the first-order terms in the leptodermous expansion give rise to a *phase shift* in the periodic orbit expansion, while the frequencies $S^{cavity}_{(\lambda,\nu)}$ are unchanged.

A. Classical action

To introduce the basic idea of the leptodermous expansion, we first consider potentials that differ from the cavity potential only in a small region around the cluster surface, say for $r>R_0-\alpha$. It is then straightforward to split the radial integrals into two parts, one integral over the interior $r=0,\ldots,R_0-\alpha$ and one over the surface region $r=R_0-\alpha,\ldots,r_{out}$. Thus the radial action can be rewritten as

$$\begin{aligned} s_r/\hbar&=\int_{r_{in}}^{r_{out}}\sqrt{E-V(r)-L^2/r^2}\,dr\\ &=\int_{r_{in}}^{R_0-\alpha}\sqrt{.}\,dr+\int_{R_0-\alpha}^{r_{out}}\sqrt{.}\,dr. \end{aligned} \tag{30}$$

The first integral is the action integral for a spherical cavity of radius $R_0-\alpha$, which we know already. The second integral can, in general, not be solved analytically. But for small α we can obtain a good approximation by neglecting the variation of the angular momentum term over the small interval $[R_0-\alpha,r_{out}]$, e.g., setting L^2/r^2 to L^2/R_0^2.

Realistic cluster potentials are not that simple. In a Woods-Saxon potential there is no obvious point that separates bulk from surface. We can still make the same ansatz by choosing some small α, but we have to make sure that our result does not depend on our specific choice. To do so, we add and subtract the integral $\int_0^{R_0-a}\sqrt{E+V_0-L^2/R_0^2}\,dr$ to Eq. (30). Using $V(r)\approx -V_0$ for $r<R_0-a$, we find

$$s_r/\hbar \approx \int_{r_{in}}^{R_0-\alpha} \sqrt{E+V_0-L^2/r^2}\,dr + \int_0^{r_{out}} \sqrt{E-V(r)-L^2/R_0^2}\,dr - \int_0^{R_0-\alpha} \sqrt{E+V_0-L^2/R_0^2}\,dr. \quad (31)$$

Using again $L^2/r^2 \approx L^2/R_0^2$ for $r \in [R_0-\alpha, r_{out}]$, we can extend the upper limit of integration of the first and third integrals from $R_0-\alpha$ to r_{out}. The first integral is then the radial action for the cavity potential, and the two other terms give the correction due to the soft surface of the potential $V(r)$. Introducing dimensionless quantities $\hat{a}=a/R_0$, $\hat{s}=s/kR_0$, and $\hat{L}=L/\hbar kR_0$, with $k=\sqrt{E+V_0}$, and expanding in powers of the reduced surface-width $\hat{a}$, we obtain

$$\hat{s}_r(P,\hat{L},\hat{a}) = \hat{s}_r^{cavity}(\hat{L}) + \hat{I}_s(P,\hat{L})\hat{a} + \mathcal{O}(\hat{a}^2), \quad (32)$$

where $P=\sqrt{(E+V_0)/V_0}$, and $\hat{s}_r^{cavity}(\hat{L}) = \sqrt{1-\hat{L}^2} - \hat{L}\arccos(\hat{L})$ is the reduced radial action for a spherical cavity. In the Appendix it is shown how to calculate $\hat{I}_s$ for a Woods-Saxon potential.

Given the expansion for the radial action, we now proceed to calculate the action for a periodic orbit (λ,ν),

$$\hat{S}_{(\lambda,\nu)} = 2\nu\hat{s}_r + 2\pi\lambda\hat{L}_{(\lambda,\nu)}. \quad (33)$$

The angular momentum $L_{(\lambda,\nu)}$ associated with the orbit can be determined from the periodicity condition: In order to close after λ turns and having traversed the outer turning point ν times, the angle Φ swept during one radial oscillation must be $\pi\lambda/\nu$. With Eq. (32), this leads to

$$\frac{\pi\lambda}{\nu} = \Phi = -\frac{\partial \hat{s}_r}{\partial \hat{L}} = \arccos(\hat{L}) - \frac{\partial \hat{I}_s}{\partial \hat{L}}\hat{a} + \mathcal{O}(\hat{a}^2). \quad (34)$$

Taking the derivative with respect to $\hat{a}$ at $\hat{a}=0$, we can solve for the first-order correction in the reduced angular momentum:

$$\hat{L}_{(\lambda,\nu)} = \hat{L}_{(\lambda,\nu)}^{cavity} - \sqrt{1-(\hat{L}_{(\lambda,\nu)}^{cavity})^2}\frac{\partial \hat{I}_s(P,\hat{L}_{(\lambda,\nu)}^{cavity})}{\partial \hat{L}}\hat{a}. \quad (35)$$

We can use this to expand $\hat{s}_r^{cavity}(\hat{L})$ in Eq. (32) around $\hat{L}_{(\lambda,\nu)}^{cavity} = \cos(\pi\lambda/\nu)$. Inserting into Eq. (33), we see that the first-order correction in $\hat{s}_r^{cavity}$ cancels that coming from $\hat{L}$. Thus to first order in $\hat{a}$ the reduced action for a periodic orbit (λ,ν) is given by

$$\hat{S}(P,\hat{L}_{(\lambda,\nu)},\hat{a}) = \hat{S}_{(\lambda,\nu)}^{cavity} + 2\nu\hat{I}_s(P,\hat{L}_{(\lambda,\nu)}^{cavity})\hat{a} + \mathcal{O}(\hat{a}^2). \quad (36)$$

This result is independent of the specific form of the potential, as long as an expansion (32) of the radial action exists.

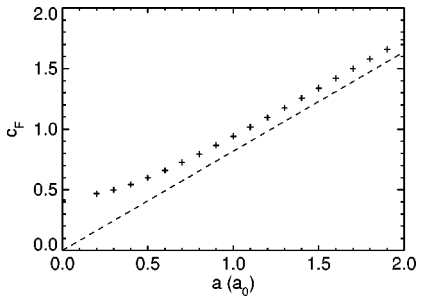

FIG. 7. Surface term c_F in the asymptotic expansion of $\overline{k_F} r_s$ [cf. Eq. (37)] as a function of the surface width a for a Woods-Saxon potential. The potential parameters are $V_0=0.45$ Ry and $r_s=4a_0$). The crosses were obtained by fitting the Fermi wave vector from full quantum-mechanical calculations for clusters with 50, . . . ,8000 electrons. The dashed line gives the estimate of c_F as given by Eq. (43).

B. Fermi level

We now turn to the problem of determining the Fermi wave vector $\overline{k_F}$ in the extended Thomas-Fermi approximation for a cluster with N electrons. In an infinite system we have $\overline{k_F} r_s = (9\pi/4)^{1/3}$. For a finite system there will be corrections arising form the surface

$$\overline{k_F} r_s = (9\pi/4)^{1/3} + c_F N^{-1/3} + \cdots . \quad (37)$$

The surface term can be calculated from the quantum-mechanical scattering phase $\varphi(k)$ at the surface potential,[33,34]

$$c_F = -\frac{3}{\overline{k_F^2}}\int_0^{\overline{k_F}} \left(\frac{\pi}{4} - \varphi(k)\right) k\, dk. \quad (38)$$

Assuming that the potential is slowly varying at the outer turning point, we can determine the scattering phase from the classical action.

For a slowly varying potential, the WKB wave function in the region $r \ll R_0 - a$, where the potential is practically constant is[31]

$$u_{WKB}(r) \propto \cos\left(\int_r^{r_{out}} k(r)\, dr - \frac{\pi}{4}\right), \quad (39)$$

while the quantum-mechanical wave function is

$$u_{QM}(r) \propto \cos[k(R_0-r) - \varphi(k)]. \quad (40)$$

In the semiclassical limit, i.e., for large R_0, both expressions should be equal. Choosing $r=0$, we find

$$\varphi(k) = -\left(\int_0^{r_{out}} k(r)\, dr - kR_0\right) + \frac{\pi}{4} \quad (41)$$

$$= \frac{\pi}{4} - \hat{I}_s(P,0)ka + \mathcal{O}(a^2), \quad (42)$$

where in the last equation we have used the linearization (32) of the radial action. We note that for $L=0$ the leptodermous expansion is exact, i.e., there are no higher-order terms in Eq. (32). From Eq. (38), the surface parameter is thus

$$c_F = -\frac{3a}{\bar{k}_F^2}\int_0^{\bar{k}_F} \hat{I}_s[P(k),0]k^2 dk \tag{43}$$

$$= -\left(\frac{9\pi}{4}\right)^{1/3} \hat{I}_N(P_F)\frac{a}{r_s}. \tag{44}$$

The analytic expression of $\hat{I}_N$ for Woods-Saxon potentials is calculated in the Appendix [Eq. (A10)].

It is interesting to note that we can obtain the same result from expanding the Thomas-Fermi integral in powers of a

$$N = \int_0^{r_{out}} [\bar{E}_F - V(R)]^{3/2} r^2 dr = \frac{(\bar{k}_F R_0)^3}{3} + (\bar{k}_F R_0)^3 \hat{I}_N \hat{a}, \tag{45}$$

and solving for $\bar{k}_F r_s$. In fact, in the approximation considered here, both approaches are equivalent.

It is important to realize that the above reasoning involves two, possibly conflicting, approximations. In ansatz (39) for the semiclassical wave function, we have assumed that the potential is slowly varying, i.e., that a is large enough, while for the leptodermous expansion of the radial action of the orbits with $L \neq 0$ we require that a is small.

To see how well expression (43) for c_F works, we compare it to the surface term obtained by fitting the Fermi wave vector $k_F(N)$ calculated quantum mechanically for Woods-Saxon potentials holding 50, . . . ,8000 electrons (see Fig. 7). As expected, our approximation approaches the quantum-mechanical result in the limit of large surface width a (slowly varying potential regime). But it also works quite well for relatively small a. For very small a the approximation of course breaks down, since our ansatz does not describe the crossover from the slowly varying potential regime to the potential step at $a=0$, for which the phase in $u_{WKB}(r)$ is $\arctan(\kappa/k)$ instead of $\pi/4$. Using this phase in the above derivation, we recover the correct surface parameter for the finite potential well.

Since for larger a the approximation to c_F runs roughly parallel to the true value of the surface term, one might improve the accuracy of the leptodermous expansion by shifting Eq. (43) by a constant (a-independent) amount c_1. Since the Woods-Saxon potential in one dimension is exactly solvable,[35,36] this is straightforward.

C. Maslov phase

For separable potentials, the Maslov phase is determined by the phases that the semiclassical wave function picks up at the classical turning points. For a given periodic orbit (λ,ν) there are 2λ turning points in the ϑ motion, each contributing a phase $\pi/2$. The same orbit also has 2ν radial turning points. The ν inner turning points ''see'' the smooth centrifugal potential, and hence also contribute $\pi/2$. The phase ϕ_{out} at the outer turning point depends on the shape of the potential $V(r)$ at the surface. The Maslov phase for the orbit is then given by

$$\varphi_{(\lambda,\nu)} = [(1/2 + \phi_{out}/\pi)\nu + \lambda - 1/4]\pi. \tag{46}$$

For a step potential, we can find ϕ_{out} by matching the semiclassical radial wave function to the boundary condition at the turning point. For an infinite potential well $\phi_{out} = \pi$, while for a well of depth V_0 $\phi_{out} = 2\arctan(\kappa/k)$, where $\kappa = \sqrt{V_0 - k^2}$. For a slowly varying potential, on the other hand, the standard result obtained by linearizing the potential around the classical turning point is $\phi_{out} = \pi/2$.

The Woods-Saxon potential for a typical cluster has a surface width of $a = 0.5 \ldots 1.5 a_0$. As we have seen above, for such values of a the potential is already in the slowly varying regime. We therefore use

$$\varphi_{(\lambda,\nu)} = [\nu + \lambda - 1/4]\pi. \tag{47}$$

D. Leptodermous POE

We can now collect all the contributions to calculate the effect of a softening of the potential at the surface on the periodic orbit expansion (25) of the oscillating part $\tilde{E}$ of the total energy. The frequencies associated with the periodic orbits turn out to be unchanged; to first order there is only a phase shift

$$\tilde{E}(N) \propto \sum_{(\lambda,\nu)} \beta_{(\lambda,\nu)} \cos\left[\left(\frac{9\pi}{4}\right)^{1/3} \hat{S}^{cavity}_{(\lambda,\nu)} N^{1/3} + \Delta\Phi_{(\lambda,\nu)}\right], \tag{48}$$

with

$$\Delta\Phi_{(\lambda,\nu)} = \left(\frac{9\pi}{4}\right)^{1/3} [2\nu \hat{I}_s(P,\hat{L}) - \hat{S}^{cavity}_{(\lambda,\nu)} \hat{I}_N(P)]\frac{a}{r_s} - [\nu + \lambda - 1/4]\pi. \tag{49}$$

We stress again that we have made two, possibly conflicting, approximations. On the one hand, the leptodermous expansion of the radial action relies on the fact that the surface width a is small, while a slowly varying potential assumption enters in the calculation of the scattering phase. To see how the above expression works in practical calculations, we compare the periodic orbit expansion (48) with the result of quantum-mechanical calculations for Woods-Saxon potentials with parameters typical for an alkali metal cluster; see Fig. 8. The agreement is surprisingly good. The shift of the supernodes with increasing surface width is well described, and also the shell oscillations are quite well reproduced. We could obtain even better agreement by numerically fitting the action integrals (see Fig. 10) and the surface coefficient c_F with *linear* functions in a. In that sense the concept of the surface introducing just a phase shift in the periodic orbit expansion seems to be applicable even beyond the range where the analytical expressions from the leptodermous expansion are good approximations.

Taking only triangular and square orbits into account, the shift in the shell (supershell) oscillations is given by $(\Delta\Phi_{(1,3)} \pm \Delta\Phi_{(1,4)})/2$. As we can see from Eq. (49), the contributions coming from c_F almost cancel for the supershells, since the classical actions for the triangular and the square orbit are so similar. Because of this cancellation of errors the shift of the supershells with the surface width is very well described in the leptodermous expansion.[16] The shell oscillations are more sensitive to approximations. But the most important feature, namely, that shells are hardly affected by changes in the surface width, is also well reproduced.

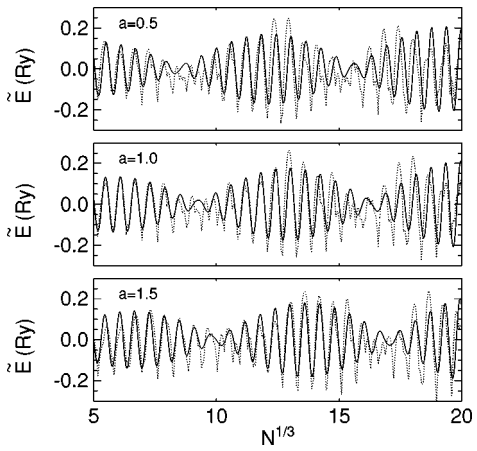

FIG. 8. Oscillating part $\tilde{E}$ of the total energy for Woods-Saxon potentials $V(r)=-V_0/(1+\exp\{[(r-R(N)]\}/a)$ with different surface width a. $R(N)=N^{1/3}r_s$ with $r_s=4a_0$ and $V_0=0.45$. The dotted lines give the results of quantum-mechanical calculations. The full lines are obtained from the leptodermous expansion (48), including only triangular and square orbits.

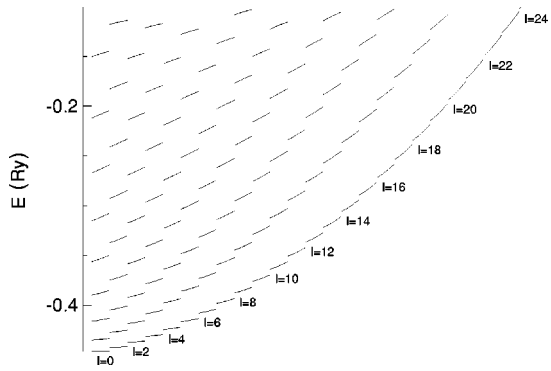

FIG. 9. Shift in the energy levels $\varepsilon_{n,l}$ for Woods-Saxon potentials with different surface width a. The parameters for the potentials are $V_0=0.45$ Ry, $R_0=50a_0$, and $a=0.5a_0,\ldots,1.5a_0$. For given angular momentum l the levels are plotted one above the other. Each line shows $\varepsilon_{n,l}$ as a function of a, with a increasing from left to right.

V. CONCLUSIONS

Using periodic orbit theory, we see that the electronic supershell structure is a sensitive probe for the surface of clusters. There is a pronounced effect of the width of the surface region on the position of the supershells. The leptodermous expansion around the limiting case of a spherical cavity provides a natural framework for understanding the shift of the supershells with increasing surface width. A particularly nice feature of the leptodermous expansion, as we have presented it here, is the fact that the expansion of the radial action is the *only* input we need. All other quantities entering the periodic orbit expansion can be easily derived from the radial action. It is therefore straightforward to apply the formalism to other types of potentials.

The shift in the electronic supershells that is described by the leptodermous expansion has been seen in numerical studies of $\tilde{E}$ for soft potentials,[28] and it has been used to understand the results of self-consistent jellium calculations.[16] The observations of a shift proportional to the surface width can be regarded as a signature of the leptodermous regime. Eventually the leptodermous approximation will break down, since for extremely soft potentials the planar orbits with $\lambda=1$ cease to exist. For such potentials star orbits become the leading terms, which causes a change in the *frequency* of the shell and supershell oscillations[37,38] as opposed to a change in the *phase* only.

It is interesting to compare the leptodermous expansion of the semiclassical sum over periodic orbits with the quantum-mechanical perturbation theory. In quantum mechanics we would expect perturbation theory to break down when the shifts of the energy levels are of the order of their spacing. For the potentials we have considered here, the change in the energy levels is quite large, especially for the levels with high angular momentum, which are most sensitive to the potential at the surface. Typical shifts of the energy levels with the surface width a for a set of Woods-Saxon potentials are shown in Fig. 9. Nevertheless, the electronic shells are not that strongly affected, because the levels with large angular momentum, which are mostly responsible for the oscillations in the total energy, are shifted by large, but similar, amounts. It seems that since the semiclassical periodic orbit expansion does not deal with individual energy levels but only with the collective changes in the spectrum, it works so well, even for large surface widths a.

The leptodermous expansion should also be of use in understanding experiments probing the transport properties of high-mobility semiconductor microstructures.[39] The oscillations in the conductance of quantum dots are quite well described by simple cavity potentials. At first sight this seems surprising, since the confining potential of a quantum dot is expected to be rather smooth. However, if these potentials are still in the leptodermous regime, it is clear that calculations using simple cavity potentials (or billiards) already describe the qualitatively correct physics.

ACKNOWLEDGMENTS

It is a pleasure to thank O. Gunnarsson for his invaluable advice. Helpful discussions with T. P. Martin and M. Brack are gratefully acknowledged. A. Burkhardt, A. Schuhmacher, and K. Rößmann did a great job supporting us with Computer Algebra Tools.

APPENDIX: LEPTODERMOUS EXPANSION FOR A WOODS-SAXON POTENTIAL

In this appendix we show how to evaluate the integrals in the leptodermous expansion for a Woods-Saxon potential (9).

1. Radial action

For a potential with small surface width a the radial action can be approximately written as [see the discussion after Eq. (31)]

$$s_r/\hbar \approx \int_{r_{in}}^{R_0} \sqrt{E+V_0-L^2/r^2}\,dr + \int_0^{r_{out}} \sqrt{E-V(r)-L^2/R_0^2}\,dr - \int_0^{R_0} \sqrt{E+V_0-L^2/R_0^2}\,dr. \quad \text{(A1)}$$

The first integral is the radial action for the spherical cavity. The third integral is trivial: the integrand is a constant. Introducing $k=\sqrt{E+V_0}$ and $\hat{L}=L/\hbar k R_0$ to simplify the notation, it is given by $\hbar k R_0\sqrt{1-\hat{L}^2}$. The second integral is more difficult. Rewriting the Woods-Saxon potential (9) as

$$V(r) = -V_0 + \frac{V_0}{2}\left[1+\tanh\left(\frac{r-R_0}{2a}\right)\right], \quad \text{(A2)}$$

and substituting $y=(r-R_0)/a$, we are led to

$$\frac{\sqrt{2}\hat{a}}{P}\int_{-1/2\hat{a}}^{\operatorname{artanh}(c)} \sqrt{c-\tanh(y)}\,dy, \quad \text{(A3)}$$

with $c=2P^2(1-\hat{L}^2)-1$, $P=\sqrt{(E+V_0)/V_0}$, and $\hat{a}=a/R_0$. This expression can be evaluated analytically:

$$2\hat{a}\left\{\sqrt{1-\hat{L}^2}\operatorname{artanh}\sqrt{\frac{1-\hat{L}^2-\dfrac{1+\tanh(-1/\hat{a})}{2P^2}}{1-\hat{L}^2}} - \sqrt{\frac{1}{P^2}-(1-\hat{L}^2)}\arctan\sqrt{\frac{1-\hat{L}^2-\dfrac{1+\tanh(-1/2\hat{a})}{2P^2}}{1/P^2-(1-\hat{L}^2)}}\right\}. \quad \text{(A4)}$$

Since the ansatz [Eq. (A1)] is already a first-order approximation, we need only the expansion of the above expression for small a. For the second term this is straightforward:

$$\arctan\sqrt{\cdot} = \arcsin(P\sqrt{1-\hat{L}^2}) + \mathcal{O}(\hat{a}^2). \quad \text{(A5)}$$

The first term is a bit more difficult, since for $\hat{a}\to 0$ the $\operatorname{artanh}\sqrt{\cdot}$ diverges as $1/2\hat{a}$. We find

$$2\hat{a}\ \operatorname{artanh}\sqrt{\cdot} = 1 + 2\hat{a}\ \ln(2P\sqrt{1-\hat{L}^2}) + \mathcal{O}(\hat{a}^2). \quad \text{(A6)}$$

Collecting our results, we see that we can expand the radial action for a Woods-Saxon potential with surface parameter a around the radial action of the corresponding spherical cavity. The term of first order in a is given by $\hat{I}_s(P,\hat{L})\hat{a}$, with

$$\hat{I}_s(P,\hat{L}) = \frac{2}{P}[P_L\ \ln(2P_L) - \sqrt{1-P_L^2}\arcsin(P_L)], \quad \text{(A7)}$$

where we have introduced $P_L = P\sqrt{1-\hat{L}^2}$.

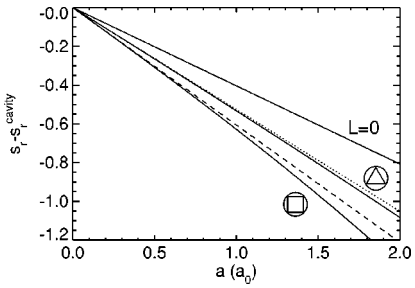

FIG. 10. Change of the radial action (in units of $\hbar$) for Woods-Saxon potentials with different surface width a. The parameters for the potential are $V_0=0.45$ Ry and $R_0=40a_0$. The full lines give the radial action $s_r(E)$ for a triangular and a square orbit. $k=(9\pi/4)^{1/3}1/r_s$. The dotted line shows the change in the radial action for the triangular orbit as calculated using the leptodermous expansion ($\hat{I}_s ka$). The dashed line shows the same for the square orbit.

To check how good this linearization of the radial action works in practice, we compare it to numerical results. Figure 10 shows such a comparison for a Woods-Saxon potential that roughly resembles a sodium cluster with 1000 electrons. As can be seen, the leptodermous expansion works quite well. It is exact for $L=0$ (which is the quantity entering in the calculation of c_F). For the triangular orbit the approximation is very good even for rather large surface widths a. For the square orbit the expansion still works well, although we start to see deviations for larger a. This is due to the fact that in the leptodermous expansion we make an approximation in the angular momentum term, which becomes more critical for orbits with large ν. It is worth noting that the change in the radial action is surprisingly linear in a. This means that we could obtain results in the spirit of the leptodermous expansion (i.e., having only phase shifts in the periodic orbit expansion), by fitting the results of numerical calculations of the action integrals with a linear function. Using such fits, we could improve the accuracy of our results.

2. Fermi level

From Eq. (43), the surface term for $\overline{k_F} r_s$ in the leptodermous expansion is given by

$$c_F = -\frac{3a}{\overline{k_F^2}}\int_0^{\overline{k_F}} \hat{I}_s(P,0)k^2\,dk. \quad \text{(A8)}$$

Inserting Eq. (A7), we find

$$c_F = -\frac{6V_0^{3/2}a}{\overline{k_F^2}}\int_0^{P_F}[P^2\ln(2P) - P\sqrt{1-P^2}\arcsin(P)]\,dP, \quad \text{(A9)}$$

with $P=k/\sqrt{V_0}$. The first integral is straightforward, and the second is easily evaluated by substituting $y=\arcsin(P)$. We thus obtain Eq. (44) with

$$\hat{I}_N(P) = 2\left(\ln(2P) + \left[\frac{1}{P^2}-1\right]^{3/2}\arcsin(P) - \frac{1}{P^2}\right). \quad \text{(A10)}$$

[1] T. P. Martin, S. Bjørnholm, J. Borggreen, C. Bréchignac, P. Cahuzac, K. Hansen, and J. Pedersen, Chem. Phys. Lett. **186**, 53 (1991).
[2] J. Pedersen, S. Bjørnholm, J. Borggreen, K. Hansen, T. P. Martin, and H. D. Rasmussen, Nature (London) **353**, 733 (1991).
[3] C. Bréchignac, P. Cahuzac, F. Carlier, M. de Frutos, and J. P. Roux, Phys. Rev. B **47**, 2271 (1993).
[4] M. Pellarin, B. Baguenard, C. Bordas, M. Broyer, J. Lermé, and J. L. Vialle, Phys. Rev. B **48**, 17 645 (1993).
[5] H. Nishioka, K. Hansen, and B. R. Mottelson, Phys. Rev. B **42**, 9377 (1990).
[6] R. Balian and C. Bloch, Ann. Phys. (N.Y.) **69**, 76 (1972).
[7] M. C. Gutzwiller, J. Math. Phys. **11**, 1791 (1970).
[8] D. E. Beck, Solid State Commun. **49**, 381 (1984).
[9] W. Ekardt, Phys. Rev. B **29**, 1558 (1984).
[10] J. Lermé, C. Bordas, M. Pellarin, B. Baguenard, J. L. Vialle, and M. Broyer, Phys. Rev. B **48**, 12 110 (1993).
[11] J. Lermé, M. Pellarin, B. Baguenard, C. Bordas, J. L. Vialle, and M. Broyer, Phys. Rev. B **50**, 5558 (1994).
[12] J. Lermé, M. Pellarin, J. L. Vialle, and M. Broyer, Phys. Rev. B **52**, 2868 (1995).
[13] J. Lermé, Phys. Rev. B **54**, 14 158 (1996).
[14] J. Lermé, M. Pellarin, E. Cottancin, B. Baguenard, J. L. Vialle, and M. Broyer, Phys. Rev. B **52**, 14 163 (1995).
[15] E. Koch and O. Gunnarsson, Phys. Rev. B **54**, 5168 (1996).
[16] E. Koch, Phys. Rev. Lett. **76**, 2678 (1996).
[17] V. M. Strutinsky, Nucl. Phys. A **122**, 1 (1968).
[18] M. Brack, J. Damgard, A. S. Jensen, H. C. Pauli, V. M. Strutinsky, and C. Y. Wong, Rev. Mod. Phys. **44**, 320 (1972).
[19] C. Yannouleas and U. Landman, Phys. Rev. B **48**, 8376 (1993).
[20] P. Stampfli and K. H. Bennemann, Phys. Rev. Lett. **69**, 3471 (1992).
[21] J. P. Perdew, Y. Wang, and E. Engel, Phys. Rev. Lett. **66**, 508 (1991).
[22] E. Engel and J. P. Perdew, Phys. Rev. B **43**, 1331 (1991).
[23] O. Genzken and M. Brack, Phys. Rev. Lett. **67**, 3286 (1991).
[24] M. Brack, Rev. Mod. Phys. **65**, 677 (1993).
[25] P. Hohenberg and W. Kohn, Phys. Rev. **136**, B864 (1964).
[26] W. Kohn and L. J. Sham, Phys. Rev. **140**, A1133 (1965).
[27] W. D. Knight, K. Clemenger, W. A. de Heer, W. A. Saunders, M. Y. Chou, and M. L. Cohen, Phys. Rev. Lett. **52**, 2141 (1984).
[28] K. Clemenger, Phys. Rev. B **44**, 12 991 (1991).
[29] M. V. Berry and K. E. Mount, Rep. Prog. Phys. **35**, 315 (1972).
[30] M. C. Gutzwiller, *Chaos in Classical and Quantum Mechanics* (Springer, New York, 1990).
[31] M. Brack and R. K. Bhaduri, *Semiclassical Physics* (Addison-Wesley, Reading, MA, 1997).
[32] For potentials with a very soft surface some orbits (λ, ν) may cease to exist (Refs. 37 and 38). Since we are not concerned with such extremely soft potentials, we do not consider that case here.
[33] R. Balian and C. Bloch, Ann. Phys. (N.Y.) **60**, 401 (1970).
[34] Ph. J. Siemens and A. Sobiczewski, Phys. Lett. B **41**, 16 (1972). The equivalence of Eq. (3) with the expression given by Balian and Bloch is seen by an integration by parts.
[35] L. D. Landau and E. M. Lifshitz, *Quantum Mechanics* (Pergamon, New York, 1977).
[36] S. Flügge, *Rechenmethoden der Quantentheorie* (Springer, Heidelberg, 1990).
[37] J. Lermé, M. Pellarin, J. L. Vialle, B. Baguenard, and M. Broyer, Phys. Rev. Lett. **68**, 2818 (1992).
[38] J. Mansikka-aho, M. Manninen, and H. Nishioka, Phys. Rev. B **48**, 1837 (1993).
[39] P. E. Lindelof, P. Hullmann, P. Bøggild, M. Persson, and S. M. Reimann, in *Large Clusters of Atoms and Molecules*, edited by T. P. Martin (Kluwer, Dordrecht, 1996), p. 89.